Scanning Microscopy Vol. 11, 1997 (Pages 323-334) 0891-7035/97$5.00+.25
Scanning Microscopy International, Chicago (AMF O'Hare), IL 60666 USA

SOLVING THE PHASE PROBLEM IN PROTEIN ELECTRON CRYSTALLOGRAPHY: MULTIPLE ISOMORPHOUS REPLACEMENT AND ANOMALOUS DISPERSION AS ALTERNATIVES TO IMAGING

Christoph Burmester and Rasmus R. Schröder*

Department of Biophysics, Max-Planck-Institute for Medical Research, Heidelberg, Germany

Abstract

Electron crystallography of 2-dimensional protein crystals combines electron diffraction with high resolution imaging of the crystals to calculate an electron density map. However, high resolution imaging is still associated with many technical problems whereas the registration of diffraction patterns to high resolution is less demanding. The ability to retrieve phase information from diffraction patterns with heavy atoms, as in X-ray crystallography, would therefore open up new vistas. Thus we have investigated both theoretically and experimentally the use of heavy atom labelling. Model calculations show that substituted heavy atoms affect electron diffraction intensities and that anomalous dispersion and multiple isomorphous replacement (MIR) are indeed potential techniques for phase determination. Since the expected changes are small the intensities of electron diffraction patterns have to be measured with sufficient accuracy. For thin catalase micro crystals we find that significant difference Patterson maps can be obtained if sensitive electron detectors and zero-loss energy filtering are used. Heavy atom derivative diffraction patterns have been recorded which show significant changes from native protein diffraction patterns.

Key Words: Electron crystallography, multiple isomorphous replacement, anomalous dispersion.

*Address for correspondence:
Rasmus R. Schröder
Department of Biophysics
Max-Planck-Institute for Medical Research
Jahnstr. 29, 69120 Heidelberg, Germany
Telephone number: +49-6221-486362
FAX number: +49-6221-486437
E-mail: Rasmus.Schroeder@mpimf-heidelberg.mpg.de

Introduction

Although electrons are much more suitable than X-rays for structure determination of very small protein crystals (Henderson, 1995; Appendix), the standard method for protein structure determination at near atomic resolution still is X-ray crystallography. Only three membrane proteins have been structurally described at molecular level by electron microscopy (Henderson *et al*., 1990; Jap *et al*., 1991; Kühlbrandt *et al*., 1994; Grigorieff *et al*., 1996). Electron crystallography is hampered by fundamental methodological problems such as: (i) the growth of suitable 2D crystals, (ii) the determination of phase information at high resolution. One possible solution to the latter problem is the adaptation of X-ray crystallographic methods for phase determination to electron crystallography, i.e., the application of the multiple isomorphous replacement or anomalous dispersion. In these approaches phase information is no longer obtained by imaging but by the evaluation of differences in diffraction patterns caused by substituted heavy atoms. Therefore, the problem of imaging with near atomic resolution is converted into the registration of diffraction patterns with high accuracy. This should be advantageous since high resolution diffraction patterns are more easily obtained than comparable images.

This alternative method for phase determination has been studied by Ceska and Henderson (1990) who came to the conclusion that in their case data of sufficient accuracy were not available. However, the use of new techniques such as improved detection devices or the removal of the inelastic background by energy filtering yields more accurate data. Here we present a new evaluation of the limits on signal detection set by the basic physical processes. This is compared with new experimental data on the detection of single heavy atoms in protein crystals to demonstrate that phase determination by multiple isomorphous replacement (MIR) is now feasible.

Scattering Theory and Physical Limits on Heavy Atom Effects

Electron diffraction

The interaction between electrons and the specimen can be described in wave formalism as the modulation of

the incident wave, i.e., the exit wave can be written as

$$\psi_s(\mathbf{r}) = a_s(\mathbf{r}) \exp(i\varphi_s(\mathbf{r}))\psi_0(\mathbf{r}) \quad (1)$$

where $\psi_0(\mathbf{r})$ = incident plane wave, $a_s(\mathbf{r})$ = absorption term, $\varphi_s(\mathbf{r})$ = phase shift, $\varphi_s(\mathbf{r})$ being proportional to the crystal potential.

The functions $a_s(\mathbf{r})$ and $\varphi_s(\mathbf{r})$ can be derived from the Schrödinger equation, which, after Fourier transformation, may be written as a set of non linear equations (for a derivation see, e.g., Cowley and Moody, 1957).

In principle, this set of equations has to be solved for the scattering potential knowing the scattering amplitudes and phases (dynamical scattering theory). Unfortunately, in general this is not possible. However, if the crystal is thin compared to the extinction length the problem simplifies (kinematic approximation) and the scattering potential can be calculated as the Fourier synthesis of the complex diffraction pattern or *vice versa*.

In the case of electron diffraction from protein crystals one records the diffraction pattern of the protein crystal in order to calculate the electron density map of the protein which is (for light atoms) approximately proportional to the potential of the specimen. This procedure presumes the validity of the kinematic approximation for the specimen under investigation. For two-dimensional (2D) protein crystals, only negligible deviations from the kinematic approximation are observed. However, caution is necessary for three-dimensional (3D) protein crystals. Specimen thickness, specimen density, unit cell dimensions and crystal mosaicity all influence the limiting thickness for the kinematic approximation. Therefore from theory alone it is almost impossible to predict the behaviour of a specimen if its structure is unknown. For this reason an experimental check is very helpful. Such a routine experimental procedure has now been developed using energy filtering techniques [described elsewhere (Burmester *et al*., in preparation)]. Relevant results are given below.

Electron scattering

For phase determination the Z-dependence of the atomic scattering factors f(θ) is important. For electron scattering, f(θ) of a Coulomb Potential is given by (cf. quantum mechanical textbooks, e.g., Messiah, 1976)

$$f(\theta) = \frac{\gamma}{2k \sin^2(\theta/2)} \exp(2i\sigma_0 - i\gamma \sin^2(\theta/2)) \quad (2)$$

$$\gamma = \pm(Ze^2m/(h/2\pi)^2k \quad (3)$$

where θ describes the scattering angle, k the wave vector, and σ_0 the total scattering cross section (*e* and *m* denote electron charge and mass, *h* denotes the Planck constant). Note that f(θ) is complex and that $|f(\theta)|$ as well as the phase of f(θ) depends on the atomic charge e*Z.

Note that:

(a) for electrons the atomic scattering factor f(θ) is not simply proportional to the atomic number as it is for X-rays since the screening effect reduces the increase of $|f(\theta)|$ with atomic number. Therefore, the average effect of a substituted heavy atom on the structure factor is smaller for electrons than for X-rays.

(b) f(θ) is complex for all elements and for all wavelengths, therefore one observes anomalous dispersion and deviation from Friedel symmetry. For so called "weak phase objects" (e.g., light atoms) it is possible to apply the Born approximation and to obtain real atomic scattering factors. Thus one does not observe anomalous dispersion for light atoms. However, the Born approximation cannot be used for atoms of high atomic numbers, instead other approximations have been developed (WKB method, Wentzel, Kramer, Brillouin; muffin tin model). From these approaches as well as from experiments complex scattering factors have been determined (Zeitler and Olsen, 1967; Raith, 1968; Reimer and Sommer, 1968; Haase, 1968; see also Ibers and Vainstein, 1962).

Multiple Isomorphous Replacement (MIR) and Anomalous Dispersion

The phase problem can in general be solved by using heavy atom derivatized crystals (see e.g., Watenpaugh, 1985). For each set of Bragg indices *hkl* the structure factor of the native form $\mathbf{F}_p$ is compared with that from a heavy atom derivative crystal $\mathbf{F}_{ph}$.

These (complex) structure factors are related to each other by

$$\mathbf{F}_{ph} = \mathbf{F}_p + \mathbf{F}_h \quad (4)$$

where $\mathbf{F}_h$ is the structure factor for the heavy atoms alone. $|\mathbf{F}_{ph}|$ and $|\mathbf{F}_p|$ are available experimentally from difference Patterson maps and the value of the (vector) $\mathbf{F}_p$ can be calculated.

In order to calculate $\mathbf{F}_h$ it is necessary to know the positions of the heavy atoms, which may be found by deconvoluting the heavy atom Patterson function (autocorrelation function). An approximation to the Patterson map of the heavy atoms alone is obtained by calculating the Patterson map of the differences between the amplitudes of the derivative crystal and the native crystal

$$\Delta P(\mathbf{r}) = (1/V) \sum_{hkl} (|\mathbf{F}_{ph}| - |\mathbf{F}_p|)^2 \cos(2\pi hr) \quad (5)$$

	X-ray		electrons	
resolution range	N ↔ A	N ↔ B	N ↔ A	N ↔ B
∞ ... 5.0Å	7.6%	10.8%	1.6%	2.4%
5.0Å ... 3.5Å	10.1%	14.3%	3.3%	4.8%
3.5Å ... 2.5Å	17.2%	27.1%	6.0%	9.9%

Table 1. Comparison of the crystallographic R_{merge}-factor for electron and X-ray scattering intensities $|\mathbf{F}|^2$ of simulated diffraction data: N = native catalase tetramer, A = Hg-derivative at position 'C' (Murthy *et al*., 1981), B = Hg-derivative with two heavy atoms bound at positions 'A' and 'C' (Murthy *et al*., 1981).

Alternatively one can determine the coordinates of the heavy atoms by using their anomalous scattering (Rossmann, 1961). Assuming that only the heavy atoms have a complex scattering factor and that all other atoms have real atomic scattering factors, one can write the atomic scattering factor as $f(\theta) = f' + if''$. The structure factor can then be written as

$$F_h = \sum_j f'_j \exp(2\pi i h r_j) + i \sum_j f''_j (\exp 2\pi i h r_j) \quad (6)$$

Now consider a structure with light atoms, which show a negligible anomalous scatterering, giving rise to a structure factor $\mathbf{F}_h(N)$. In addition, there are a few heavy atoms with strong anomalous scattering, with a non anomalous component and the anomalous component

$$\mathbf{F}''_h(H) = i(f''/f')\,\mathbf{F}_h(H) \quad (7)$$

The total structure factor will be $\mathbf{F}_h$. Then we get

$$|\mathbf{F}''_h(H)|^2 = (1/4)(|\mathbf{F}_h| - |\mathbf{F}_{-h}|)^2 \quad (8)$$

hence a Patterson map with coefficients $(|\mathbf{F}_h| - |\mathbf{F}_{-h}|)^2$ will be equivalent to a Patterson map with coefficients $|\mathbf{F}''_h(H)|^2$ which is proportional to $|\mathbf{F}_h(H)|^2$. This will be a Patterson map with vectors between all anomalous scatterers and can thus be used to find the heavy atom positions. Knowing the positions of the heavy atoms, the value of the (vector) $\mathbf{F}_h$ can be calculated by triangulation in the complex plane (Harker construction).

However, one needs to be able to detect small effects. Therefore we first estimate what the effect of heavy atoms will be on the Friedel-symmetry (using the crystallographic R-factor R_{sym}) and on the diffraction intensities (R_{merge}). For the discussion of the anomalous dispersion one has in addition to check first, whether the assumption that only the heavy atoms can be treated as anomalous scatterers and the light atoms as real scatterers is valid for electron diffraction. As second point one has to estimate the effect of heavy atoms on the Friedel symmetry R_{sym}.

Model Calculations

To quantify the effects of MIR and anomalous dispersion molecular structure factors have been calculated using complex atomic structure factors (Rose, 1977) for both the known atomic model of catalase tetramers in the case of R_{merge} and a statistical model protein (625 C, 195 O, 175 N, 3 S, and 2P atoms; randomized atomic coordinates, see Table 2 and Figure 3 for details) in the case of R_{sym}. Table 1 gives the expected magnitudes of effects expressed in the crystallographic R-factors R_{merge} as a measure of the similarity of diffraction patterns.

The effect of heavy atom substitution on diffraction intensities has been calculated by Crick deriving general formulas for the intensity changes depending on the atomic scattering factors (Crick and Magdoff, 1956). These relations are applicable to electron diffraction, the expected effect is for electrons about a third of that for X-rays (cf. atomic scattering factors for electrons and X-rays, e.g., International Tables). As is shown in Table 1 the same effect can be observed in the crystallographic R-factor.

To estimate the effect of anomalous dispersion, the molecular structure factors of a model protein with 1000 atoms have been calculated for X-rays and electrons. Table 2 gives the deviation from Friedel symmetry in terms of the crystallographic R-factor R_{sym}.

Note that the effect of the anomalous scattering for

	resolution range			
	∞ ... 5.0Å	5.0Å ... 3.5Å	3.5Å ... 2.5Å	∞ ... 2.5Å
protein (1000 atoms)	0.77%	0.84%	1.28%	0.90%
protein + 1 Hg	4.87%	6.69%	9.26%	6.33%
protein + 2 Hg	8.56%	11.55%	15.20%	10.90%

Table 2. Friedel symmetry R_{sym}-factor as calculated from simulated diffraction intensities taking into account anomalous scattering. As "protein" a typical distribution of C-, O-, N-, S-, and P-atoms was used (1000 atoms using randomized position coordinates in a 50x50 $Å^2$ projection area; 625 C, 195 O, 175 N, 3 S, 2P).

electron diffraction is higher than in the case of isomorphous replacement (cf. Table 1). This is in contrast to X-rays, which in general show a weaker multiple anomalous diffraction signal compared to MIR. In fact, the nature of the anomalous scattering is completely different for X-rays and electrons. In the case of X-rays atoms show anomalous dispersion only if the X-ray energy is close to that of absorption edges. In contrast to that, in the case of electrons all atoms show anomalous dispersion at all electron energies. However, light atoms as weak scatterers have negligible complex scattering factors, i.e., proteins composed of light atoms only are well described by the Born approximation leading to real scattering factors. Only when heavy atoms are added - as for a possible phase determination - anomalous dispersion will be observed (cf. Table 2, native vs. Hg derivative).

Comparing R_{merge}-factors between X-ray and electron diffraction for MIR it is obvious that utilizing MIR in electron diffraction will be more difficult than for X-rays. However, to judge the feasability of this approach it is necessary to take into account not only the average criteria R_{sym} and R_{merge}, but also the expected absolute and relative intensity changes for X-ray and electron diffraction when adding single heavy atoms. Corresponding results for the above model calculations are shown in Figures 1 and 2: Adding heavy atoms to a protein structure leads for both X-rays and electrons to changes which are almost identical in their characteristic behaviour. Note that in both cases the changes show a wide spread of relative changes to more than 200%, while the average behaviour in R-factors (cf. Table 1) gives only a change of about 4-6% [electron microscopy (EM)] and 10-17% (X-ray). The expected differences should be detectable in the EM case since especially the weak Bragg intensities, which could cause statistical problems in their accurate intensity measurement, show the highest relative changes, whereas small relative changes are more frequent for the well defined, high intensity Bragg reflections.

Experimental Approach

In this section we present data from thin 3D catalase crystals as model system. We are reporting data on the limiting thickness for kinematic scattering, on detection accuracy, and on the need for classification of diffraction patterns according to crystal absorption and isomorphism to avoid systematic errors. Finally, the first results on the detection of single heavy atoms are presented. The data are presented in detail elsewhere (Burmester and Schröder, in preparation; Burmester *et al*., in preparation).

Materials and Methods

A suspension of bovine liver catalase crystals (Serva, Heidelberg, Germany; 61312 U/mg) was centrifuged and the pellet then dissolved in 20% NaCl, 0.04% NaN_3. The catalase solution was dialyzed against a 30 mM phosphate-buffer at pH 6.3. Every 12h a quarter of the buffer was replaced by pure water. After a few days crystals appeared, as judged by the silkiness of the solution. After 4 days the dialysis was stopped and the crystal suspension was stored at 4°C.

Heavy atom derivative crystals. Crystals in the crystal suspension were allowed to sediment, then the solvent was removed and replaced by a 5 mM phosphate buffer at pH 6.3. The buffer contained 50 mM K_2PtCl_4 for the Pt derivatives and 0.05 mM $HgCl_2$ for the Hg derivative. The crystals were soaked for 30 min (Pt derivative) or for 3 h (Hg derivatives), then applied on a carbon film grid and flash-frozen in liquid ethane.

Soaking conditions are similar to the conditions used by Murthy *et al*. (1981) so that reproducable heavy atom binding to the catalase tetramer can be assumed. The

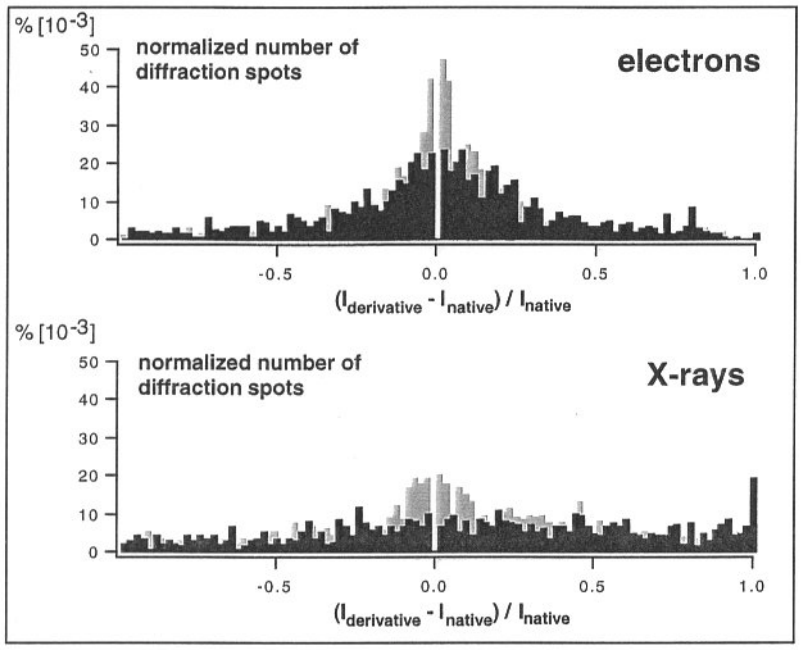

Figure 1. Comparison of intensity change distributions for electrons and X-ray diffraction. For each *hkl* the expected diffraction spot intensity was calculated using the catalase tetramer coordinates as "native" and the Hg-derivative at position 'C' (Murthy *et al*., 1981) as "derivative" (grey bars). Adding a second Hg atom leads to larger relative changes for both X-ray and electron scattering (positions 'A' and 'C' of Murthy *et al*., 1981, black bars).

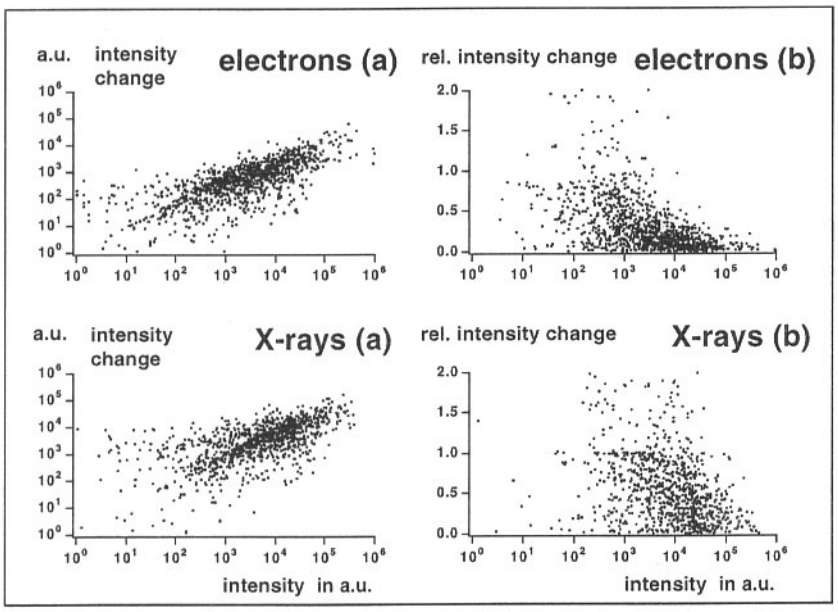

Figure 2. Comparison of intensity change distributions for electrons and X-ray diffraction. As in Figure 1 diffraction spot intensities were calculated using the native protein and a single Hg-derivative. (**a**) shows the absolute intensity changes vs the diffraction spot intensities, (**b**) shows the relative intensity changes vs the diffraction spot intensities. Note that the overall characteristics of the heavy atom effect is quite comparable. In the case of X-rays the averaged effect is about 3 times larger than for electrons.

differences in soaking time follow from the higher accessability of the potential binding sites by diffusion for the thin microcrystals used here as compared to the thick macroscopic crystals used for X-ray studies.

All electron diffraction patterns were recorded using a LEO (Oberkochen, Germany) EM 912 Omega at 120keV electron energy. Specimens were held at a temperature of -170°C in the EM using an Oxford Instruments (Oxford, UK) Cryo Transfer System CT3500Z. In the case of zero loss filtered images and diffraction patterns the energy width of the filter was set to 25 eV. The exposure was carried out under low dose conditions with a dose of 2 $e^-/Å^2$. For diffraction patterns the camera length was 2900 mm, using an illumination aperture of 0.04 mrad. All diffraction patterns were recorded on Fuji Imaging Plates (Fuji Photo Film Co., Osaka, Japan). The Imaging Plates were scanned at a pixel resolution of 37.5 * 37.5 μm^2 using the scanner described by Burmester *et al*. (1994a).

All computer processing was done using a set of new programs developed for a Convex C2 (Convex, Richardson, TX) and Silicon Graphics (SGI, Mountain View, CA) workstations.

α	$\Sigma I_{significant}/I_D$	$\lvert I_{thin}-I_{thick}\rvert/I_D$	N/N_D
0.1	14.7%	8.2%	3.9%
0.05	6.0%	3.5%	1.8%
0.025	3.9%	2.4%	0.7%

Table 3. Diffraction intensities from thin and thick catalase crystals classified according to three significance levels (α=0.1, 0.05 and 0.025 in the t-test). Compared are the sums of significantly changed Bragg diffraction intensities and the intensity changes as percentage of the total intensity. N: number of significantly changed diffraction spots, N_0: total number of diffraction spots in a complete pattern, I_0: total intensity in a complete pattern. Comparison of the two columns shows that stronger diffraction spots dominate the overall changes. This can be explained by the higher signal to noise/background ratio of such spots leading to a higher significance in the t-test. However, at the 5% level for thick crystals (> 150nm), there is only a few % change in intensity. (Number of diffraction patterns in the two classes was 13)

Crystal thickness

As has been discussed above, one prerequisite for a quantitative evaluation of diffraction patterns is the validity of kinematical scattering theory together with the weak phase-object approximation, i.e., the typical sample thickness has to be smaller than the extinction length.

To determine the validity range of the kinematic approximation in a direct experiment one would have to vary crystal thickness continuously and to determine the thickness dependence of the intensities for each of the Bragg reflections. In this case the kinematic approximation is valid as long as all reflections show the same dependence on changes in crystal thickness. This approach is very time consuming and experimentally almost impossible, e.g., for 2D-crystals. Therefore, it is more appropriate to use an indirect measure.

It is assumed that for a given biological object multiple elastic scattering can be neglected if there is no measurable contribution to the diffraction pattern from the more probable inelastic-elastic plural scattering. This approximation is only valid for light atoms where the inelastic cross sections are much higher than the elastic cross sections (in the case of ice-embedded biological objects, cf. Angert *et al*., 1996). To show the applicability of the kinematic approximation for a given specimen it is thus sufficient to show that multiple inelastic scattering does not contribute substantially. Fortunately, the effects of multiple scattering can be detected spectroscopically, e.g., by the shift of the most probable energy loss to higher energies, contributions to Bragg intensities from inelastically scattered electrons (inelastic-elastic multiple scattering, inelastically filtered diffraction), or from the electron energy loss (EEL) spectrum for each Bragg reflexion as observed in the energy dispersive plane of an energy filtering transmission electron microscope (EFTEM), thus giving an easy routine check to validate the kinematic approximation (Burmester *et al*., in preperation).

All the above arguments are valid for weak phase objects (e.g., thin protein crystals) but they are violated if heavy atoms are added, since these atoms are strong scattering objects. Therefore, it might be questionable to use this approach to derivative crystals. However, model calculations comparing conventional scattering factors and the results of using a multi-slice algorithm (Dinges and Rose, 1995) show that the error in using the weak phase-object approximation for derivative crystals is negligible. This is illustrated in Figure 3 where difference Patterson maps of a model protein (cf. Table 2) with and without a heavy atom calculated in the two different approximations are compared. Only minor differences can be detected.

The spectroscopic methods show that a shift of the most likely energy loss in EEL spectra does not occur for crystals with thickness < 70 nm but that a shift is detectable for thicker specimens. This finding is in agreement with the observation of Bragg reflection intensities in inelastically filtered diffraction patterns (energy loss > 25 eV) for thick specimens only. Moreover, the same result is obtained by measuring the spectra of Bragg reflections which were recorded in the energy dispersive plane of the LEO EM 912 Omega. These findings show that for crystals with a thickness < 70 nm the kinematic approximation is valid.

We have used a further experimental approach to substantiate these results. According to the above, a crystal of thickness < 70 nm obeys the kinematic approximation and thus can be described as thin. We now compare these with crystals of 140-175 nm thickness, where dynamic scattering effects could become visible. Classifying

diffraction patterns according to the crystal thickness and averaging Bragg reflection intensities within each group, one arrives at two average data sets, one for thin crystals and one for thick crystals, which are then scaled with respect to each other. Using these data sets, one can apply a t-test between these two average data sets to find those reflections which have significant changes in their intensities as a function of crystal thickness. The results, given in Table 3, show that crystal thickness does indeed affect the intensities. However, only about 2% of the total number of reflections (typically in the order of 5000) show a significant change. As would be expected these reflections are in general strong, as can be seen from the fact that their intensities contribute to 6% of the total intensity. Thus the overall change of the intensity between the thin and thick crystal class contributes only to 3.5% of the overall intensity in the diffraction pattern. Since the dynamic effects between crystals of thickness < 70 nm and 140-175 nm is only 3.5% of the overall intensity, the dynamic effect for crystal thickness < 70 nm should be negligible. This result is in good agreement with the spectroscopic measurements, which indicated that one could treat crystals with a thickness of < 70 nm as kinematic scatterers.

Detection accuracy

As has been discussed above the changes in the Bragg intensities which need to be observed for MIR are small and the application of the method necessitates high detection accuracy. As is shown in Appendix 1 the achievable accuracy of the intensities should be 0.2-0.3% on average (standard deviation), which is more than adequate. However, nobody has so far reported such a high accuracy for protein crystals. The reasons for the lack of accuracy are likely to include: the use of detectors with low detection quantum efficiency; the difficulty of correcting for background in the presence of the high inelastic background; and the inherent variability of crystal packing, crystal order, crystal thickness or absorption contrast effects.

As is described in Burmester *et al.* (1994b) the use of zero-loss energy filtering to remove the inelastic background combined with imaging plates (IP) as a high definition detection system (Burmester *et al*., 1994a) allows a significant improvement on the accuracy to which diffraction patterns can be recorded. One measure for this accuracy is the R_{sym} factor for zero-tilt catalase diffraction patterns (*h0l*) which on account of being a centric projection do not show anomalous diffraction. Overall factors of about 7% have been obtained. R_{sym} can drop to 5% for favorable resolution shells, indicating the potential of the experimental method.

The fact that at present the patterns were not classified prior to averaging over patterns from different crystals is readily observed in the R-factor for merging different patterns. As is demonstrated in Table 5, the R_{merge} factor of individual patterns is still very high. However, this factor drops dramatically if classes of averages are merged, indicating that the source of the difference between individual patterns is not systematic error but arises from statistical variability in the specimens as is indicated above. This problem of variability has to be solved by improved specimen preparation. Thus it will be necessary to increase uniformity of crystals in the crystallization process. In addition, embedding ice layers must be controlled to reduce absorption effects. Finally, during data processing, classification of crystals and diffraction patterns has to be included.

Discussion: Is It Possible to Retrieve Phase Information by MIR and Anomalous Scattering Effects?

An answer can be given combining the physical constraints and the experimental results described above. One prerequisite for MIR is that heavy atoms are “heavy”, i.e., that there is an increase of the scattering cross sections with atomic number Z. It has been argued that screening effects in the case of electron diffraction would reduce the differences in cross sections. This is true, the effect of heavy atoms on intensities are indeed 3 times smaller for electron diffraction than for X-ray diffraction (cf. Table 1). However, the remaining effect is still adequate. Furthermore, atoms induce a phase shift of the scattered wave which also increases with atomic number Z. Model calculations showed that this phase shift gives no significant anomalous dispersion for native protein crystals, but does induce a significant anomalous component for heavy atom derivative crystals (cf. Table 2).

From these results we conclude that it should be possible to use MIR and anomalous scattering for phase determination in electron diffraction. It is shown in appendix 1 that even for micro crystals the theoretical statistical limit on accuracy is better than 1% (standard deviation). This has to be compared with the expected changes from MIR (Tables 1 and 2) of the order of 5 % - 10%. In an ideal experimental setup with no noise and no background MIR should work well even for microcrystals. Thus, it is necessary to consider the real experimental situation with its sources of signal degradation.

Ceska and Henderson (1990) showed that there are considerable problems in achieving an accuracy as high as expected from Poisson statistics. Possible reasons for their difficulties could have been limitations in the detection process and the high background signal due to inelastically scattered electrons. Recently, new detection techniques have overcome the limitations of negative film as a detector. Moreover, energy filtered microscopes now offer the

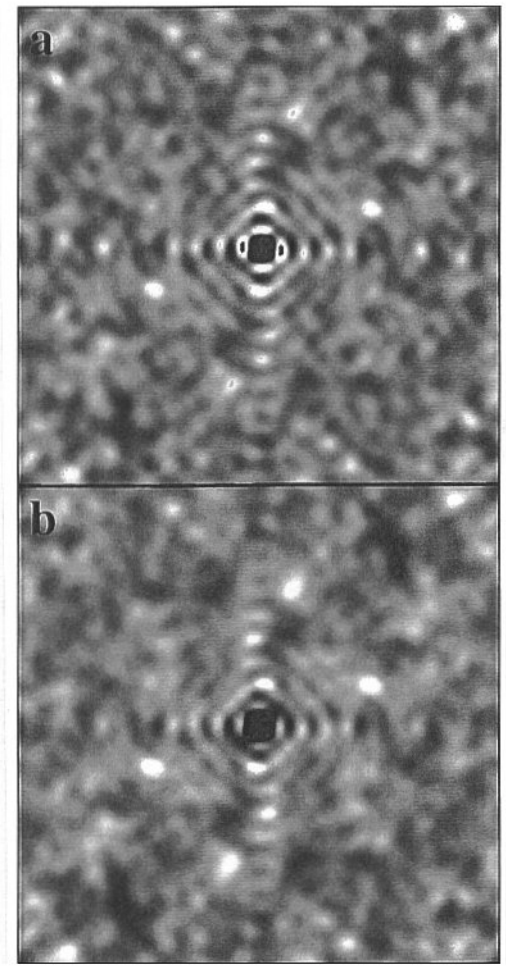

Figure 3. Difference Patterson maps of a model protein (1000 atoms, 50x50 Å^2 area, 1 Å thickness) with and without one heavy atom (Hg) as calculated (**a**) using a multislice algorithm without the assumption of weak phase scattering factors (Dinges and Rose, 1995) and (**b**) using vector sums over weak phase scattering factors. Shown is the unit cell Patterson map P(± 0.5, ± 0.5, 0). Note that there are no changes in the maxima positions indicating the validity of the weak phase object approximation.

possibility of removing the high background level due to inelastically scattered electrons. Using a combination of imaging plates and zero energy loss electron diffraction we have obtained diffraction patterns with much higher accuracy as measured by the statistical factors R_{sym} (Table 4) and R_{merge} (Table 5, last column). This accuracy should already be sufficient to allow one to observe the effects of added heavy atoms (cf. Tables 1 and 2) and indeed a first result has been achieved: there are significant changes in the electron diffraction patterns between native catalase crystals and Hg and Pt derivatives as shown in Figure 4.

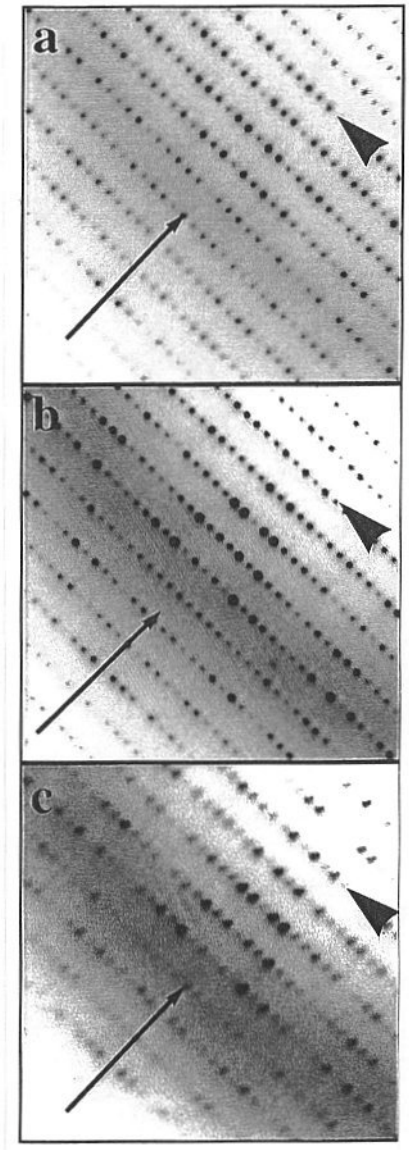

Figure 4. Details of catalase electron diffraction patterns recorded from frozen hydrated samples at 120 keV electron energy using Imaging Plates at a LEO EM 912 energy filtering TEM (original data, no background subtraction or averaging). (**a**) native crystals, (**b**) Hg-derivative, and (**c**) Pt-derivative. The arrows indicate the (*h00*) direction, the arrowhead points to the (*14,0,l)* order which corresponds in the detail shown to ca 3.5Å resolution. Note the differences in the diffraction patterns which prove to be significant at 5 % t-test level.

As is described in detail elsewhere (Burmester *et al.*, in preparation) the relative intensity changes seen in Figure 4 can be quantified and tested for their statistical significance. In these tests it becomes clear that the intensity

resolution range			
> 2.5Å	> 5.0Å	5.0Å ... 3.5Å	3.5Å ... 2.5Å
7.7%	7.9%	7.2%	8.5%
7.0%	5.1%	6.3%	16.0% *

Table 4. Crystallographic R_{sym}-factor of two typical diffraction patterns (frozen hydrated catalase crystals, experimental details as described in text).

resolution range	N = 20	N = 20	N = 2
∞ ... 5.0Å	29.9%	32.8%	8.4%
5.0Å ... 3.5Å	19.1%	23.7%	4.2%
3.5Å ... 2.5Å	16.5%	22.1%	4.5%

Table 5. Crystallographic R_{merge}-factors for catalase diffraction patterns (frozen hydrated catalase crystals, experimental details as described in text) for 2 arbitrary subgroups of patterns (number of patterns N=20) and the two averaged subgroups (N=2). The relatively high R_{merge} for individual patterns (N=20) shows the high variability of individual patterns. However, the small R_{merge}-factor for averaged subgroups indicates that there are no systematic but statistical variations (see text) which can be overcome by averaging larger numbers of diffraction patterns.

changes between native and derivative data are not dominated by the observed variability of individual diffraction patterns as revealed by relatively large R_{merge} factors. Instead, comparing patterns classified as native, Pt-derivative, or Hg-derivative within one class as well as between different classes shows that differences between native and derivative patterns are substantially stronger than those of patterns within one class. Therefore an unambiguous detection of heavy atom effects is shown.

However, the fact that individual diffraction patterns do vary considerably shows that the situation is far from ideal. This is reflected in the high R_{merge} factors of individual patterns as shown in column 1 and 2 of Table 5. Fortunately this variability is due to factors such as imperfect crystal preparation, absorption and contrast effects. Another potential problem could be small crystal tilting, which in this study has been excluded by classifying patterns according to systematic variations of the Friedel symmetry. All these effects lead to increased R_{merge} factors between individual diffraction patterns, nevertheless, the effects do average out for very large data sets. The achievable accuracy is within the needed range and can be further improved by averaging over diffraction patterns from different crystals (cf. columns 1, 2 and 3 in Table 5). Experimentally, the effects of heavy atom derivatives are readily detectable (Fig. 3). The next steps on the way to structure determination without imaging will be the classification of diffraction patterns according to crystal thickness, crystal quality, or crystal preparation combined with the averaging of larger numbers of patterns. Furthermore, recent results on the determination of pattern orientation in three dimensions (Dimmeler *et al.*, 1996) indicate that such averaging will be possible in 3 dimensions as well, using large numbers of patterns from tilted crystals.

From the discussion above it is clear that now - as for X-ray - new problems emerge. The possible usage of crystallographic methods in electron diffraction sets new constraints on the quality and reproducibility of protein crystals (native and derivatives). Also it will be necessary to collect very large numbers of data sets to allow classifications and averaging. Furthermore - just as in X-ray - not every heavy atom derivative can be used for phase determination, its phasing power will depend, e.g., on the actual protein binding sites. One more recent aspect of electron diffraction studies includes direct phasing and phase extension studies (Dorset, 1995). Here it could be

advantageous to get better defined scattering factor amplitudes and use the phases obtained by MIR as starting phases for refinement steps. These problems have now to be investigated further.

Acknowledgements

The authors would like to thank K.C. Holmes for constant encouragement and support as well as many helpful discussions. This work was supported in part by the Deutsche Forschungsgemeinschaft (grants Schr 424-1/1, Schr 424-1/2).

Appendix: Comparison of the Necessary Number of Crystal Unit Cells for EM and X-ray Studies

Radiation damage is caused by energy transfer due to inelastic scattering. To obtain a high signal/noise ratio the ratio between elastic and inelastic scattering cross sections and the average energy transfer per inelastic scattering event are relevant. For X-ray scattering, the ratio inelastic/elastic scattering cross section is about 10 and the average energy transfer per inelastic event is about 8000 eV, which gives an energy deposition of 80 keV per elastic scattering event. In contrast, in electron scattering the ratio inelastic/elastic is about 3 and there is on average only 20 eV transferred in an inelastic scattering event, thus giving only 60 eV energy deposition per elastic event (see also Henderson, 1995).

Let us assume that the crystal can tolerate a maximum energy deposition of E_{max}/nm^3 which is equivalent to $N_{max}*V$ scattering events each depositing an energy E_{dep} if V is the volume of the crystal and N_{max} is the number of scattering events per volume element with $N_{max}*E_{dep} = E_{max}$. If we want to achieve a certain signal to noise ratio SNR in a diffraction pattern, we need to have an average of $N = SNR^2$ elastic scattering events per Bragg reflection (Poisson statistics). A given N_{max} value defines the minimum crystal volume V which is necessary to obtain the given signal to noise ratio. From the numbers given above one finds that for electron diffraction the volume of a crystal can be smaller by a factor of approx. 1000 compared to X-ray (also see Henderson, 1995).

In the experiments discussed an illuminated area of 22.9 μm^2 has been used, which was fully covered by the catalase crystals. Experiments have shown that for vitrified catalase 3D micro-crystals the resolution of 2 Å is preserved for a dose of 2 $e^-/Å^2$. With an illuminated area of 22.9 μm^2 we have a total dose of $4.6 * 10^9$ electrons. With a crystal thickness of at least 17.5 nm (unit cell thickness) and a mean elastic scattering cross section of approx. 100 nm, approx. 16% of the electrons are scattered elastically. Having roughly 7000 Bragg reflections in a diffraction pattern image this gives approx. $1.1*10^5$ electrons per Bragg reflection, which gives a standard deviation of 0.2-0.3 % on average. To give an additional lower limit on the effect consider the weakest spots which are typically in the order of 10^3 electrons leading to a standard deviation of 2-3%. This will be the limit to observe the discussed MIR effects (cf. Table 1). It should be noted, however, that the weaker spots tend to show high relative changes due to substituted heavy atoms.

References

Angert I, Burmester C, Dinges C, Rose H, Schröder RR (1996) Elastic and inelastic scattering cross-sections of amorphous layers of carbon and vitrified ice. Ultramicroscopy **63**: 181-192.

Burmester C, Braun HG, Schröder RR (1994a) A new quasi-confocal image plate scanner with improved spatial resolution and ideal detection efficiency. Ultra-microscopy **55**: 55-65.

Burmester C, Holmes KC, Schröder RR (1994b) Electron-diffraction patterns from frozen hydrated protein microcrystals: A new tool in structural studies. Proc 52nd Ann Meeting Microsc Soc America. Bailey GW, Garrott-Reed AJ (eds). San Francisco Press, San Francisco. pp. 102-103.

Ceska TA, Henderson R (1990) Analysis of high resolution electron diffraction patterns from purple membrane labelled with heavy atoms. J Mol Biol **213**: 539-560.

Cowley JM, Moody AF (1957) The scattering of electrons by atoms and crystals. I. A new theoretical approach. Acta Cryst **10**: 609-619.

Crick FHC, Magdoff BS (1956) The theory of the method of isomorphous replacement for protein crystals. I. Acta Cryst **9**: 901-908.

Dimmeler E, Burmester C, Schröder RR (1996) Determination of diffraction spot profiles in electron crystallography of 3D protein crystals. Proc 11th Eur Congress Electron Microsc Dublin. Comm Eur Soc Microsc, Bruxelles. Vol. III, pp 8-9.

Dinges C, Rose H (1995) Simulation of filtered and unfiltered TEM images and diffraction patterns. Phys Stat Sol (A) **150**: 23-33.

Dorset DL (1995) Comments on the validity of the direct phasing and Fourier methods in electron crystallography. Acta Cryst **A51**: 869-879.

Grigorieff N, Ceska TA, Downing KH, Baldwin JM, Henderson R (1996) Electron-crystallographic refinement of the structure of bacteriorhodopsin. J Mol Biol **259**: 393-421.

Haase J (1968) Berechnung der komplexen Streufaktoren für schnelle Elektronen unter Verwendung von Hartree-Fock-Atompotentialen (Calculation of complex

scatteering factors for fast electrons using Hartree-Fock atom potentials). Z Naturforsch **A23**: 1000-1019.

Henderson R (1995) The potential and limitations of neutrons, electrons and X-rays for atomic resolution microscopy of unstained biological material. Quart Rev Biophys **28**: 171-194.

Henderson R, Baldwin JM, Ceska TA, Zemlin F, Beckmann E, Downing KH (1990) Model for the structure of bacteriorhodopsin based on high-resolution electron crystallography. J Mol Biol **213**: 899-929.

Ibers JA, Vainshtein BK (1962) Scattering amplitudes for electrons. In: International Tables for X-Ray Crystallography, Vol. 3. Lonsdale K (ed). Kynoch, Birmingham. pp 216-226.

Jap BK, Walian PJ, Gehring K (1991) Structural architecture of an outer membrane channel as determined by electron crystallography. Nature (London) **350**: 167-170.

Kühlbrandt W, Wang DN, Fujiyoshi Y (1994) Atomic model of plant light-harvesting complex by electron crystallography. Nature (London) **367**: 614-621.

Messiah A (1976) Quantum Mechanics, Vol 1. North-Holland, 9th edition. Chapter XI.

Murthy MRN, Reid III TJ, Sicignano A, Tanaka N, Rossmann MG (1981) Structure of beef liver catalase. J Mol Biol **152**: 465-499.

Raith H (1968) Komplexe Atomstreuamplituden für die elastische Elektronenstreuung an Festkörperatomen (Complex atom scattering amplitudes for elastic electron scattering against solid state atoms). Acta Cryst **A24**: 85-93.

Reimer L, Sommer KH (1968) Messungen und Berechnungen zum elektronenmikroskopischen Streukontrast für 17 bis 1200 keV-Elektronen (Measurements and calculations on electron microscopical scattering contrast for 17-1200 keV electrons). Z Naturforsch **A23**: 1569-1582.

Rose H (1977) Nonstandard imaging methods in electron microscopy, Ultramicroscopy **2**: 251-267.

Rossmann MG (1961) The position of anomalous scatterers in protein crystals. Acta Cryst **14**: 383-388.

Watenpaugh KD (1985) Overview of phasing by isomorphous replacement. Methods Enzymol **115**: 3-15.

Zeitler E, Olson H (1967) Complex scattering amplitudes in elastic electron scattering. Phys Rev **162**: 1439-1447.

Discussion with Reviewers

Reviewer I: In the appendix you claim a detection accuracy of 0.2-0.3 % should be achievable, but in the experimental approach section you give the experimentally observed accuracies, with your top quality detection system as high as 5-7 %. What do you think are the main reasons for this large discrepancy? Do you think you will be able to reach an accuracy close to the expected theoretical limit?
Authors: From our experimental data we learned that the most critical step for obtaining a uniform data distribution was the preparation of crystals and microscope samples. This includes crystal mosaicity, crystal thickness, the removal of excess water layers around the crystal, and crystal orientation (see below). One way to be very selective for "good" data is the classification of diffraction patterns and the rejection of any pattern showing deviations in intensities deriving, e.g., from absorption effects. To finally reach very high accuracy it will be necessary to improve the methods for specimen preparation and data selection.

Reviewer II: The concept of anomalous scattering in electron diffraction is not well known. Please comment.
Authors: It has long been neglected that atoms do have complex atomic scattering factors [cf. the references to Raith (1968), Reimer and Sommer (1968) and Zeitler and Olson (1967)]. In fact, for the normal biological sample consisting of light atoms anomalous scattering is not a major effect, as we demonstrate in Table 2. This situation changes drastically if heavy atom labels are added to the protein. Comparison of Tables 1 and 2 shows that the effect of anomalous scattering on the crystallographic R-factor is at least comparable if not stronger than the normal effect of the stronger real scattering factor. From our experimental experience it is much too early to give any final answer but it might well prove that for electron diffraction evaluating anomalous scattering will lead to a higher phasing power than MIR.

Reviewer I: With regard to the crystallographic R factors, do you think crystal orientation is also an important factor?
Authors: Yes, we do. To test this we performed simulations on modelled 2D and 3D crystals. These tests showed that small deviations from the ideal zero tilt can not be detected for monolayered crystals. For multilayered, 3D crystals even tilt angles much smaller 1° show detectable effects in the patterns. We did not elaborate on this so far, since for our current experimental data crystal orientation seems not to be the main error. This follows from a simple analysis of the dependence of R_{sym} with resolution: in the model calculations R_{sym} is strongly dependent on resolution, which is not observed in this way for the experimental data (cf. Table 4). We conclude that other errors - like crystal mosaicity etc - still dominate our data. Nevertheless, for finally applying our ideas to really solve unknown structures it will be crucial to determine tilt angles very accurately and first steps in this direction are done (cf. Dimmeler *et al.*, 1997).

Additional Reference

Dimmeler E, Holmes KC, Schröder RR (1997)

Determination of tilt parameters in electron diffraction patterns of 3-D microcrystals. Proc 55th Ann Meeting Microsc Soc America. Bailey GW (ed). Springer, New York. pp 1081-1082.